Polytropic models of filamentary interstellar clouds – II. Helical magnetic fields

Claudia Toci[1] and Daniele Galli[2]⋆

[1]*Dipartimento di Fisica e Astronomia, Università degli Studi di Firenze, via G. Sansone 1, I-50019 Sesto Fiorentino, Italy*
[2]*INAF-Osservatorio Astrofisico di Arcetri, Largo E. Fermi 5, I-50125 Firenze, Italy*

ABSTRACT

We study the properties of magnetized cylindrical polytropes as models for interstellar filamentary clouds, extending the analysis presented in a companion paper. We formulate the general problem of magnetostatic equilibrium in the presence of a helical magnetic field, with the aim of determining the degree of support or compression resulting from the magnetization of the cloud. We derive scale-free solutions appropriate to describe the properties of the envelopes of filaments at radii larger than the flat-density region. In these solutions, the polytropic exponent determines the radial profiles of the density and the magnetic field. The latter decreases with radius less steeply than the density, and field lines are helices twisted over cylindrical surfaces. A soft equation of state supports magnetic configurations that preferentially compress and confine the filament, whereas in the isothermal limit the field provides support. For each value of the polytropic exponent, the Lorentz force is directed outwards or inwards depending on whether the pitch angle is below or above some critical value which is a function of the polytropic exponent only.

Key words: magnetic fields – ISM: clouds.

1 INTRODUCTION

In a companion paper (Toci & Galli 2015, hereafter Paper I), we have analysed the structure and stability of unmagnetized cylindrical polytropes, the simplest possible models of interstellar filaments, with the aim of interpreting the observations recently obtained at submillimetre wavelengths by the *Herschel Space Observatory* in a sample of nearby giant molecular clouds. With respect to more complex simulations, polytropic models have the advantage of requiring the minimum number of physical constants (like the system's entropy K) and dimensionless parameters (like the polytropic exponent $\gamma_p = 1 + 1/n$ and the adiabatic exponent γ). In Paper I, in analogy with previous studies of spherical clouds and cores, we found that the observed radial density profiles of filaments are well reproduced by a narrow range of γ_p ($1/3 \lesssim \gamma_p \lesssim 2/3$) corresponding to negative values of the polytropic index n. In particular, a good fit is obtained with $\gamma_p \approx 1/2$ ($n \approx -2$), the polytropic exponent that characterizes the pressure of a superposition of low-amplitude undamped Alfvén waves. It is of interest, therefore, to investigate further the properties of magnetized filaments.

Starting from the work of Chandrasekhar & Fermi (1953), several models have been proposed to study the structure and sta-

bility of filaments threaded by poloidal and/or toroidal magnetic fields (Nagasawa 1987; Fiege & Pudritz 2000) or perpendicular to the main axis (Tomisaka 2014). Unfortunately, there are few observational constraints on the strength and/or morphology of the magnetic field within filaments. Polarization observations of background stars in the optical and near-infrared suggest that the field is generally uniform and perpendicular to the filament, as, for example in the Serpens South cloud imaged by Sugitani et al. (2011) and the B211/B213/L1495 region in Taurus (Palmeirim et al. 2013). However, this is not a general rule. For example, in the Taurus cloud, the field inferred by optical polarization is oriented mainly perpendicular to the main filaments B216 and B217 (Moneti et al. 1984; Goodman et al. 1992), whereas the L1506 filament is almost parallel to the direction of the field (Goodman et al. 1990). Indications of the presence of helical magnetic field twisted along the filament's axis have been inferred in the dense core L1512 in Taurus (Falgarone, Pety & Phillips 2001; Hily-Blant et al. 2004) and in NGC 2024 in Orion B (Matthews, Fiege & Moriarty-Schieven 2002), but the evidence is often indirect (see Gahm et al. 2006 and references therein for a discussion of rotationally and magnetically twisted filaments). A survey of filamentary molecular clouds in Gould's Belt has shown that these clouds tend to be oriented either parallel or perpendicular to the ambient field direction in a bimodal fashion (Li et al. 2013), a result that, if confirmed, indicates that the formation of these structures is magnetically controlled. It should

⋆ E-mail: galli@arcetri.astro.it

be kept in mind, however, that optical and near-infrared polarization measurements do not probe the magnetic field associated with the densest parts of the filaments (Goodman et al. 1992).

Given the potentially important but still uncertain role played by the magnetic field in determining the observable properties of filamentary clouds, in this paper we examine the properties of magnetized polytropes in cylindrical geometry, focusing in particular on the conditions for force balance in the radial direction. The models presented in this paper are magnetostatic by design. The underlying idea is that the evolution of real filaments can be analysed, as a first step, as a series of magnetostatic solutions as filaments accrete more material from the surrounding environment. As discussed in Paper I, such a description does not necessarily imply a zero-velocity field everywhere, as long as the accretion speed becomes either subsonic or directed mostly parallel to the filament's axis in the central parts of the filament.

The paper is organized as follows: in Section 2, we derive the equations for the equilibrium of a cylindrical cloud with a polytropic equation of state and a magnetic field containing both a poloidal and toroidal component; in Section 3, we solve these equations in some special cases and we generalize results found in previous studies; in Section 4, we present scale-free semi-analytical solutions applicable the power-law envelopes of filamentary clouds; finally, in Section 5, we summarize our conclusions.

2 MAGNETIZED ENVELOPES

In a cylindrical system of coordinates, we consider the equilibrium structure of a self-gravitating filament threaded by a helical magnetic field with poloidal and toroidal components $\boldsymbol{B}_{\mathrm{p}}$ and B_φ defined in terms of the scalar functions $\Phi(\varpi, z)$ and $\Psi(\varpi, z)$, respectively:

$$\boldsymbol{B}_{\mathrm{p}} = \nabla \times \left(\frac{\Phi}{2\pi\varpi} \, \hat{\boldsymbol{e}}_\varphi \right), \qquad B_\varphi = \frac{\Psi}{2\pi\varpi}. \tag{1}$$

Following Paper I, we assume a polytropic equation of state,

$$p = K\rho^{\gamma_{\mathrm{p}}}, \tag{2}$$

where K is a constant and $\gamma_{\mathrm{p}} = 1 + 1/n$ is the polytropic exponent. The equation of magnetostatic equilibrium is

$$-\nabla V + \frac{1}{\rho}\nabla p + \boldsymbol{F}_{\mathrm{L}} = 0, \tag{3}$$

where V is the gravitational potential, related to the gas density ρ by Poisson's equation

$$\nabla^2 V = 4\pi G\rho, \tag{4}$$

and

$$\boldsymbol{F}_{\mathrm{L}} \equiv \frac{1}{4\pi\rho}(\nabla \times \boldsymbol{B}) \times \boldsymbol{B} \tag{5}$$

is the Lorentz force per unit mass. With the definitions (1), the Lorentz force becomes

$$\boldsymbol{F}_{\mathrm{L}} = -\frac{1}{16\pi^3\rho\varpi^2}[\mathcal{S}(\Phi)\nabla\Phi + \Psi\nabla\Psi + \nabla\Phi \times \nabla\Psi], \tag{6}$$

where $\mathcal{S}$ is the Stokesian operator

$$\mathcal{S}(\Phi) = \frac{\partial^2\Phi}{\partial\varpi^2} + \frac{\partial^2\Phi}{\partial z^2} - \frac{1}{\varpi}\frac{\partial\Phi}{\partial\varpi}. \tag{7}$$

The condition of no Lorentz force in the azimuthal direction is $\nabla\Phi \times \nabla\Psi = 0$, which implies $\Psi = \Psi(\Phi)$. The Lorentz force then reduces to

$$\boldsymbol{F}_{\mathrm{L}} = -\frac{1}{16\pi^3\rho\varpi^2}\left[\mathcal{S}(\Phi) + \Psi\frac{\mathrm{d}\Psi}{\mathrm{d}\Phi}\right]\nabla\Phi, \tag{8}$$

This generalizes the expression derived by Lizano & Shu (1989) in the case of a poloidal field (see also Li & Shu 1996 and Galli et al. 1999). Taking the dot product of the force equation (3) with $\boldsymbol{B}$ one obtains the condition of force balance along field lines

$$V + (1 + n)K\rho^{1/n} = H(\Phi), \tag{9}$$

where $H(\Phi)$ is the Bernoulli constant. The condition of force balance across field lines (along $\nabla\Phi$) is

$$-\frac{1}{16\pi^3\rho\varpi^2}\left[\mathcal{S}(\Phi) + \Psi\frac{\mathrm{d}\Psi}{\mathrm{d}\Phi}\right] = \frac{\mathrm{d}H}{\mathrm{d}\Phi}, \tag{10}$$

and Poisson's equation (4) then becomes

$$\frac{1}{\varpi}\frac{\partial}{\partial\varpi}\left[\varpi\left(\frac{\mathrm{d}H}{\mathrm{d}\Phi}\frac{\partial\Phi}{\partial\varpi} - \frac{1+n}{n}K\rho^{-1+1/n}\frac{\partial\rho}{\partial\varpi}\right)\right] +$$
$$\frac{\partial}{\partial z}\left(\frac{\mathrm{d}H}{\mathrm{d}\Phi}\frac{\partial\Phi}{\partial z} - \frac{1+n}{n}K\rho^{-1+1/n}\frac{\partial\rho}{\partial z}\right) = 4\pi G\rho. \tag{11}$$

Equations (8) and (10) show that $H(\Phi)$ is a potential for the Lorentz force, $\boldsymbol{F}_{\mathrm{L}} = \nabla H(\Phi)$.

The two coupled PDEs (10) and (11) are the two fundamental equations of the problem. To obtain a solution, one must specify the two functions $H(\Phi)$ and $\Psi(\Phi)$, and apply appropriate boundary conditions. The arbitrariness in the choice of the functional dependence of H and Ψ on the flux function Φ is a consequence of neglecting the dynamical evolution of the cloud. The loss of information on the previous evolution of the cloud results in the appearance of arbitrary functions that have to be determined from physical considerations (see e.g. Shu 1992). Although in principle any choice of H and Ψ is allowed, not all solutions would lead to a physically meaningful model for a magnetized filamentary cloud. Unfortunately, the origin of filamentary clouds in the interstellar medium (ISM) is not well understood (see discussion in Paper I), and any attempt made to reduce the arbitrariness in equations (10) and (11) must be necessarily ad hoc.

2.1 Non-dimensional equations

Equations (10) and (11) are generally valid under azimuthal symmetry. As a first simplification, we also assume cylindrical symmetry ($\partial/\partial z = 0$), reducing the problem to the solution of a system of two coupled ordinary differential equations. We define a non-dimensional radius ξ and density θ as in Paper I:

$$\varpi = \varpi_0\xi, \qquad \rho = \rho_{\mathrm{c}}\theta^n, \tag{12}$$

where

$$\varpi_0 = \left[\frac{\mp(1+n)K}{4\pi G\rho_{\mathrm{c}}^{1-1/n}}\right]^{1/2} \tag{13}$$

is the radial scalelength. Here, as in Paper I, the subscripts 'c' and 's' indicated quantities evaluated at the centre and the surface of the filament, respectively. We also define the non-dimensional magnetic flux ϕ, enthalpy h and toroidal flux function ψ as

$$\Phi = \left[\frac{\mp\pi(1+n)^3 K^3}{G^2\rho_{\mathrm{c}}^{1-3/n}}\right]^{1/2}\phi, \tag{14}$$

$$\frac{\mathrm{d}H}{\mathrm{d}\Phi} = \left[\frac{\mp G^2 \rho_{\mathrm{c}}^{1-1/n}}{\pi(1+n)K}\right]^{1/2} \frac{\mathrm{d}h}{\mathrm{d}\phi}, \tag{15}$$

$$\Psi = \left[\frac{\mp 2\pi(1+n)K\rho_{\mathrm{c}}^{1/n}}{G^{1/2}}\right]\psi, \tag{16}$$

Here and in the following, as in Paper I, the upper (lower) sign is for $n \leq -1$ ($n > -1$), where n is the polytropic index.

In non-dimensional form, the components of the magnetic field are

$$B_z = B_0 b_z, \qquad B_\varphi = B_0 b_\varphi, \tag{17}$$

where the scale factor B_0 is

$$B_0 = [\mp 4\pi(1+n)p_{\mathrm{c}}]^{1/2}. \tag{18}$$

The field components are then

$$b_z = \frac{1}{\xi}\frac{\mathrm{d}\phi}{\mathrm{d}\xi}, \qquad b_\varphi = \frac{\psi}{\xi}. \tag{19}$$

Similarly, the forces per unit volume acting on the system are: the pressure gradient,

$$-\frac{1}{\rho}\nabla P = \pm F_0 \frac{\mathrm{d}\theta}{\mathrm{d}\xi}\,\hat{\boldsymbol{e}}_\varpi, \tag{20}$$

the Lorentz force

$$\boldsymbol{F}_{\mathrm{L}} = F_0 \frac{\mathrm{d}h}{\mathrm{d}\xi}\,\hat{\boldsymbol{e}}_\varpi, \tag{21}$$

and the gravitational force

$$-\nabla V = -F_0 \left(\frac{\mathrm{d}h}{\mathrm{d}\xi} \pm \frac{\mathrm{d}\theta}{\mathrm{d}\xi}\right)\hat{\boldsymbol{e}}_\varpi, \tag{22}$$

where the scale factor F_0 is

$$F_0 \equiv [\mp 4\pi(1+n)Gp_{\mathrm{c}}]^{1/2} = G^{1/2}B_0. \tag{23}$$

With the definitions (12)–(16), equations (10) and (11) can be written in non-dimensional form

$$-\frac{1}{\xi^2\theta^n}\left[\left(\frac{\mathrm{d}^2\phi}{\mathrm{d}\xi^2} - \frac{1}{\xi}\frac{\mathrm{d}\phi}{\mathrm{d}\xi}\right)\frac{\mathrm{d}\phi}{\mathrm{d}\xi} + \psi\frac{\mathrm{d}\psi}{\mathrm{d}\xi}\right] = \frac{\mathrm{d}h}{\mathrm{d}\xi}, \tag{24}$$

and

$$\frac{1}{\xi}\frac{\mathrm{d}}{\mathrm{d}\xi}\left[\xi\left(\frac{\mathrm{d}h}{\mathrm{d}\xi} \pm \frac{\mathrm{d}\theta}{\mathrm{d}\xi}\right)\right] = \theta^n. \tag{25}$$

For the magnetic field to be well-behaved near the axis of the cylinder, equation (24)–(25) must be solved under the boundary conditions $\theta(0) = 1$ and $\mathrm{d}\theta/\mathrm{d}\xi(0) = 0$, as in Paper I, plus the conditions $\xi^{-1}\mathrm{d}\phi/\mathrm{d}\xi \to \mathrm{const.}$ and $\xi^{-1}\psi \to 0$ for $\xi \to 0$, corresponding to $B_z(0) = \mathrm{const.}$ and $B_\varphi(0) = 0$.

From equations (21) and (24), one sees that in order to provide support to the cloud an axial field must decrease with radius, whereas a toroidal field must decrease with radius more rapidly than ϖ^{-1}. Thus, in general the ability of a magnetic field to support (or to compress) a filamentary cloud depends on the radial profile of its strength and on the relative importance of the poloidal and toroidal components.

3 SPECIAL SOLUTIONS

3.1 Force-free fields

In general, magnetic force-free configurations have been applied to the study of solar prominences, where the pressure gradients and self-gravity of the plasma can be neglected with respect to the Lorentz force. The possibility that force-free configurations can also arise in the ISM has been raised by Carlqvist, Kristen & Gahm (1998) to explain the twisted appearance of some filamentary clouds on the basis of the argument that only for a nearly force-free geometry the electromagnetic effects are not too disruptive.

For $h = 0$, the magnetic configuration is force-free, and the equations for the density and the magnetic field are decoupled. Equation (24) becomes an equation only for the field,

$$\left(\frac{\mathrm{d}^2\phi}{\mathrm{d}\xi^2} - \frac{1}{\xi}\frac{\mathrm{d}\phi}{\mathrm{d}\xi}\right)\frac{\mathrm{d}\phi}{\mathrm{d}\xi} + \psi\frac{\mathrm{d}\psi}{\mathrm{d}\xi} = 0, \tag{26}$$

and equation (25) reduces to the ordinary Lane–Emden equation. Several solutions of equation (26) are known. For example, if $\psi = 0$ (poloidal field) the only regular solution is $\phi = A\xi^2$, with A arbitrary constant, corresponding to the trivial case of a uniform axial field. If $\psi = k\phi$, with k constant, equation (26) is linear and reduces to Bessell's equation with solution $\phi = C\xi J_1(k\xi)$, where $J_1(k\xi)$ is the Bessel function of the first kind of order 1 and C is a constant. In this case, $b_z = CkJ_0(k\xi)$ and $b_\varphi = CkJ_1(k\xi)$. This is Lundquist's solution (Lundquist 1950). The field lines are helices that reverse direction and handedness, since Bessell's functions are oscillatory. The Lundquist solution is one of a class of solutions with oscillatory behaviour that can be generated assuming a power-law dependence of ψ on ϕ and solving the resulting non-linear equation (Low & Lou 1990).

In the following, we limit our analysis to the case $\phi > 0$. Although in general the flux function ϕ may change sign at one or more radii, resulting in field reversals, the large-scale magnetic field threading a molecular cloud core is expected to be the result of a smooth distortion (i.e. without field reversals) of the relatively uniform field characteristic of giant molecular clouds and galactic discs.

3.2 Constant-β solutions

An axial field proportional to the square root of the gas pressure, such that the plasma $\beta_z = (8\pi p/B_z^2)^{1/2}$ is spatially constant, is a simple case to analyse because the total pressure is just a scaled-up version of the gas pressure. In this case, equations (24) and (25) reduce to

$$\frac{1+\beta_z^{-1}}{\xi}\frac{\mathrm{d}}{\mathrm{d}\xi}\left(\xi\frac{\mathrm{d}\theta}{\mathrm{d}\xi}\right) = \pm\theta^n. \tag{27}$$

With the scaling transformation $\xi \to (1 + 1/\beta_z)^{-1/2}\xi$, this is the ordinary Lane–Emden equation for unmagnetized polytropic cylinders. Thus, the analysis of Paper I remains valid, with the spatial lenght-scale ϖ_0 (and the core radius ϖ_{core}) increased by the factor $(1 + 1/\beta_z)^{1/2}$ (Talwar & Gupta 1973; Sood & Singh 2004). In particular, for all values of the polytropic index n, the mass per unit length and its critical or maximum value determined in Paper I are increased by the factor $1 + 1/\beta_z$. The same is not true in general for a purely toroidal field: only for an isothermal equation of state a toroidal field with uniform $\beta_\varphi = (8\pi p/B_\varphi^2)^{1/2}$ produces a simple rescaling of the Lane–Emden equation (Stódołkiewicz 1963). Therefore, if $\gamma_{\mathrm{p}} = 1$ the Stódołkiewicz–Ostriker density profile (see Paper I) remains valid in the presence of a helical magnetic field with constant β_z and β_ϕ. These scaled isothermal configurations have been studied by Nakamura, Hanawa & Nakano (1993).

3.3 Fiege and Pudritz's models

Fiege & Pudritz (2000) solved the equations of magnetostatic equilibrium for cylindrical clouds with an isothermal ($\gamma_p = 1$) or logotropic ($\gamma_p = 0$) equation of state. They assumed a specific functional dependence of the magnetic field strength on density and radius, namely

$$B_z = \Gamma_z \rho, \qquad B_\varphi = \Gamma_\varphi \varpi \rho, \qquad (28)$$

with Γ_z, Γ_φ being arbitrary constants. This choice is equivalent to the assumption that the ratio of magnetic flux to mass per unit length is the same in all cylindrical shells of the filament and that the toroidal component of the field is generated by a uniform twisting of the filament through a fixed angle. In our formalism, equation (28) is equivalent to

$$\frac{d\Phi}{d\varpi} = 2\pi\Gamma_z\varpi\rho, \qquad \Psi = 2\pi\Gamma_\varphi\varpi^2\rho. \qquad (29)$$

Substituting these expressions in equations (10) and (11), we obtain

$$-\frac{1}{4\pi}\left[\Gamma_z^2\frac{d\rho}{d\varpi} + \Gamma_\varphi^2\frac{d}{d\varpi}(\varpi^2\rho)\right] = \frac{dH}{d\varpi}, \qquad (30)$$

and

$$\frac{1}{\varpi}\frac{d}{d\varpi}\left[\varpi\left(\frac{dH}{d\varpi} - \frac{1+n}{n}K\rho^{-1+1/n}\frac{d\rho}{d\varpi}\right)\right] = 4\pi G\rho. \qquad (31)$$

Equation (30) can be integrated:

$$H = -\frac{1}{4\pi}\left(\Gamma_z^2\rho + \Gamma_\varphi^2\varpi^2\rho\right) + \text{const.}, \qquad (32)$$

and equation (31) can be written as

$$\frac{1}{\varpi}\frac{d}{d\varpi}\left\{\varpi\frac{d}{d\varpi}\left[H - (1+n)K\rho^{1/n}\right]\right\} = 4\pi G\rho. \qquad (33)$$

Equations (32) and (33) generalize equation D5 and D7 of Fiege & Pudritz (2000). The problem is reduced to the solution of the second order ordinary differential equation (33) for $\rho(\varpi)$, with H given by equation (32). These generalized Fiege & Pudritz (2000) models have an asymptotic power-law behaviour at large radii depending on the polytropic index n,

$$B_z \propto \rho \propto \varpi^{2n/(1-n)}, \qquad B_\varphi \propto \varpi\rho \propto \varpi^{(1+n)/(1-n)}. \qquad (34)$$

Thus, the magnetic field becomes asymptotically dominated by the toroidal component decreasing as a power-law with exponent between -1 and 0. Such toroidal field has the effect of compressing the cloud (as shown in Section 2).

4 CENTRAL CORES AND ENVELOPES OF MAGNETIZED FILAMENTS

4.1 Series expansion for small radii

On the filament's axis, symmetry requires the toroidal component of the electric current to vanish, and the axial current to be finite. This implies that, to the lowest order for $\xi \to 0$, both ϕ and ψ must decrease at least like ξ^2. A series expansion

$$\phi \approx \phi_2\xi^2 + \phi_4\xi^4 + \cdots, \qquad \psi \approx \psi_2\xi^2 + \cdots, \qquad (35)$$

gives

$$b_z \approx b_{0z} + b_{2z}\xi^2 + \cdots, \qquad b_\varphi \approx b_{1\varphi}\xi + \cdots \qquad (36)$$

with $b_{0z} = 2\phi_2$, $b_{2z} = 4\phi_4$, $b_{1\varphi} = \psi_2$. The substitution in equations (24) and (25) of the expansions (35) and the expansion for θ

$$\theta \approx 1 \pm \frac{1}{4}\xi^2 + \cdots \qquad (37)$$

gives the Lorentz force per unit mass near the axis,

$$F_L = -4F_0(b_{0z}b_{2z} + b_{1\varphi}^2)\xi + \cdots, \qquad (38)$$

where $F_0 > 0$ is given by equation (23). In any realistic model for filamentary clouds where the axial magnetic field decreases with radius following the density, the product $b_{0z}b_{2z}$ is negative, and the Lorentz force associated with the poloidal field is directed outwards, providing support to the cloud. Conversely, the Lorentz force associated with the toroidal field is directed inwards, squeezing the cloud. The behaviour of the density near the axis is $\rho/\rho_c \approx 1 - (\varpi/\varpi_{\text{core}})^2 + \cdots$, where

$$\varpi_{\text{core}} \approx \frac{2\varpi_0}{[\mp n(1 + 4b_{0z}b_{2z} + 4b_{1\varphi}^2)]^{1/2}}. \qquad (39)$$

The core radius is therefore increased by the poloidal field ($b_{0z}b_{2z} < 0$) and decreased by the toroidal field ($b_{1\varphi}^2 > 0$). This result can be used to constrain the strength and the morphology of the magnetic field near the filament's axis. As shown in Paper I, the core radius predicted by unmagnetized polytropic models is

$$\varpi_{\text{core}} \approx 0.047 \left(\frac{\sigma_c}{0.26\,\text{km s}^{-1}}\right)\left(\frac{n_c}{2 \times 10^4\,\text{cm}^{-3}}\right)^{-1/2}\,\text{pc.} \qquad (40)$$

For example, a toroidal field in the core region such that $b_{1\varphi}^2 \approx 1$ (corresponding to $B_{\varphi,c} \approx \pi G^{1/2}\varpi\rho_c$ in physical units) would reduce the core radius by a factor of ~ 2. Field strengths of this order are invoked in the models of Fiege & Pudritz (2000).

4.2 Scale-free solutions for large radii

To explore in the characteristics of polytropic magnetized filaments at large radii (say, at radii much larger than the core radius given by equation 39), we seek asymptotic solutions of equations (10) and (11) without making specific assumption on the magnetic field profile, except a power-law behaviour. Recalling that a power-law behaviour of the density in cylindrical polytropes is only possible for $n \leq -1$, in the following we restrict our analysis to this range of n.

For scale-free solutions, dimensional analysis requires $|\boldsymbol{B}| \propto G^{1/2}\rho\varpi$. In addition, the enthalpy H and the toroidal field function Ψ must have the following power-law dependence on Φ:

$$\frac{dH}{d\Phi} = H_0\left[\frac{G^2}{\pi|1+n|^nK^n}\right]^{1/(3-n)}\Phi^{-(1-n)/(3-n)}, \qquad (41)$$

$$\Psi\frac{d\Psi}{d\Phi} = 4\alpha^2\left[\frac{\pi^{2(2-n)}G^{1+n}}{(1+n)^{2n}K^{2n}}\right]^{1/(3-n)}\Phi^{(1+n)/(3-n)}, \qquad (42)$$

where H_0 is a dimensionless constant that measures the deviation of the poloidal field from force-free, α^2 is a constant measuring the strength of the toroidal field with respect to the poloidal field. In non-dimensional form, with the definitions (12)–(16), these expressions become

$$\frac{dh}{d\phi} = H_0\phi^{-(1-n)/(3-n)}, \qquad (43)$$

and

$$\psi\frac{d\psi}{d\phi} = \alpha^2\phi^{(1-n)/(3-n)}, \qquad (44)$$

Equations (43) and (44) can be integrated to give

$$h(\phi) = H_0 \left(\frac{3-n}{2} \right) \phi^{2/(3-n)}, \tag{45}$$

and

$$\psi(\phi) = \pm\alpha \left(\frac{3-n}{2} \right)^{1/2} \phi^{2/(3-n)}, \tag{46}$$

The system (24)–(25) allows power-law solutions,

$$\phi = \phi_0 \, \xi^{(3-n)/(1-n)}, \qquad \theta^n = \theta_0^n \, \xi^{2n/(1-n)}, \tag{47}$$

with the scale factors $\phi_0 > 0$ and $\theta_0 > 0$ given by

$$\frac{(3-n)(1+n)}{(1-n)^2}\phi_0^{(2(2-n))/(3-n)} + \alpha^2\phi_0^{2/(3-n)} = -H_0\theta_0^n, \tag{48}$$

$$H_0 \frac{2(3-n)}{(1-n)^2}\phi_0^{2/(3-n)} + \frac{4}{(1-n)^2}\theta_0 = \theta_0^n. \tag{49}$$

In these scale-free models, all forces (gravity, pressure gradient, and Lorentz force) decrease with radius with the same power-law slope. The Lorentz force is

$$\boldsymbol{F}_{\mathrm{L}} = H_0 \left(\frac{3-n}{1-n} \right) \phi_0^{2/(3-n)} \xi^{(1+n)/(1-n)} \hat{\boldsymbol{e}}_\varpi. \tag{50}$$

and is directed inwards for $H_0 < 0$ and outwards for $H_0 > 0$. For $H_0 = 0$, the magnetic field is force-free. In this case, the density is given by the unmagnetized scale-free solution

$$\theta^n = \left[\frac{(1-n)^2}{4} \right]^{n/(1-n)} \xi^{2n/(1-n)}, \tag{51}$$

(see equation 12 of Paper I), and the components of the field are

$$b_z = \phi_0 \left(\frac{3-n}{1-n} \right) \xi^{(1+n)/(1-n)}, \tag{52}$$

$$b_\varphi = \pm\alpha\phi_0^{2/(3-n)} \left(\frac{3-n}{2} \right)^{1/2} \xi^{(1+n)/(1-n)}. \tag{53}$$

Thus, the magnetic field lines are helices twisted over cylindrical flux tubes. The magnetic field decreases with radius with a behaviour intermediate between ξ^{-1} for an isothermal equation of state, and ξ^0 for a logatropic equation of state. For the values of the polytropic index derived in Paper I from fitting the radial density profiles, $-3 \lesssim n \lesssim -3/2$, the slope of the magnetic field is in the range from -0.2 to -0.5. Thus, following the discussion of Section 2, for all values of $n \leq -1$ the axial field always supports the cloud and the toroidal field always compresses it. The net effect then depends on the relative strength of the two components, determined by the value of the pitch angle δ (the angle between B_z and B_φ)

$$\tan\delta = \frac{|B_\varphi|}{|B_z|} = \frac{\alpha(1-n)}{[2(3-n)]^{1/2}}\phi_0^{-(1-n)/(3-n)}. \tag{54}$$

For small δ, the field is almost axial, and supports the envelope with a Lorentz force directed outwards. Increasing δ the toroidal component becomes larger, squeezing the cloud with a Lorentz force directed inwards. At some particular δ_{ff} the two effects cancel out, and the field is force-free ($H_0 = 0$). This happens when

$$\alpha = \alpha_{\mathrm{ff}} = \frac{[-(3-n)(1+n)]^{1/2}}{1-n}\phi_0^{(1-n)/(1+n)}, \tag{55}$$

as can be obtained from equation (48) setting $H_0 = 0$. Thus, for each n, the field becomes force-free when the pitch angle is

$$\tan\delta_{\mathrm{ff}} = \left(-\frac{1+n}{2} \right)^{1/2}, \tag{56}$$

a value that depends only on the polytropic index. For $n = -1$ (logatropic case) the force-free field is a poloidal field with uniform strength, while for $n \to -\infty$ (isothermal case) the force-free field is toroidal and decreases as ϖ^{-1}. For the values of n derived in Paper I for filamentary cloud, δ_{ff} varies between $26°$ and $45°$.

Fig. 1 shows the loci of solutions in the ϕ_0–θ_0^n plane (field strength versus density in non-dimensional units), for three values of the polytropic index: $n = -1.01$ (quasi-logatropic equation of state), $n = -2$ (best-fitting value for the observed filaments, see Paper I) and $n = -5$ (quasi-isothermal equation of state). Each line is a locus of solutions with a fixed value of the pitch angle δ. The parameter space is divided in two regions by the $H_0 = 0$ line of force-free configurations: for $H_0 > 0$ the Lorentz force is directed outwards and supports the cloud; for $H_0 < 0$ the Lorentz force is directed inwards and has the opposite effect. For $H_0 = 0$ the field is force-free, the pitch angle takes the value δ_{ff} given by equation (56) and the density the value given by equation (51) independently on the field strength ϕ_0 (dashed lines in Fig. 1). The line $\delta = 0$ shows the locus of solutions with a purely poloidal field. This line originates from the unmagnetized solution $\theta_0^n = [(1-n)^2/4]^{n/(1-n)}$, $\phi_0 = 0$, and lies always in the $H_0 > 0$ region of the diagram, indicating that a pure poloidal magnetic field can only support, not compress, a cloud. The solutions with $\delta = 0$ are characterized by a density scale θ_0^n larger than the density scale of the unmagnetized model, due to the extra support provided by the field. No solutions are possible above the $\delta = 0$ line.

The curves in Fig. 1 show that for an increasing field strength ϕ_0, configurations with a fixed pitch angle lower than the critical value δ_{ff} support increasingly larger densities; whereas if the pitch angle is larger than δ_{ff}, any increase in the field strength reduces the density that can be supported. However, in the latter case, equilibrium configuration only exists below a maximum value of ϕ_0. Thus, for a given field strength, there is always at least one solution with density larger than the unmagnetized solution, a pitch angle $\delta < \delta_{\mathrm{ff}}$ and magnetic effects dominated by the poloidal component ('magnetic support'), and one (or two, or zero) solutions with density lower than the unmagnetized solution, pitch angle $\delta > \delta_{\mathrm{ff}}$, and magnetic effects dominated by the toroidal component ('magnetic compression'). As shown by Fig. 1, if the equation of state is soft (upper panel) the largest fraction of parameter space is occupied by 'magnetic compression' solutions; conversely, for a quasi-isothermal equation of state (lower panel) 'magnetic support' solutions become dominant. This shows that the role of the magnetic field depends sensitively not only on the pitch angle but also on its dependence on radius via the polytropic exponent γ_{p}.

The two cases $n = 1.01$ and $n = -5$ in Fig. 1 illustrate the behaviour of the solutions approaching the logatropic and the isothermal limit, respectively. In the former case, solutions where the magnetic field provides support progressively disappear. Already for a pitch angle δ larger than about $4°$, the hoop stresses of the toroidal field dominate over the extra support of the dominant poloidal field, squeezing the cloud. Accordingly, the density is lower than that of the unmagnetized solution. Increasing $-n$, the region with $H_0 < 0$ shrinks, and the transition from support to compression occurs at larger pitch angle (about $35°$ for $n = -2$). For $n = -5$, the allowed parameter space is largely populated by solutions where the field provides support to the filament ($H_0 > 0$), but in the limit $n \to -\infty$ the region of no solutions covers the entire ϕ_0–θ_0^n plane. The unmagnetized solution tends to $\theta_0^n = 0$ in this limit. In fact, even in the unmagnetized case, no scale-free solution exists for an isothermal equation of state.
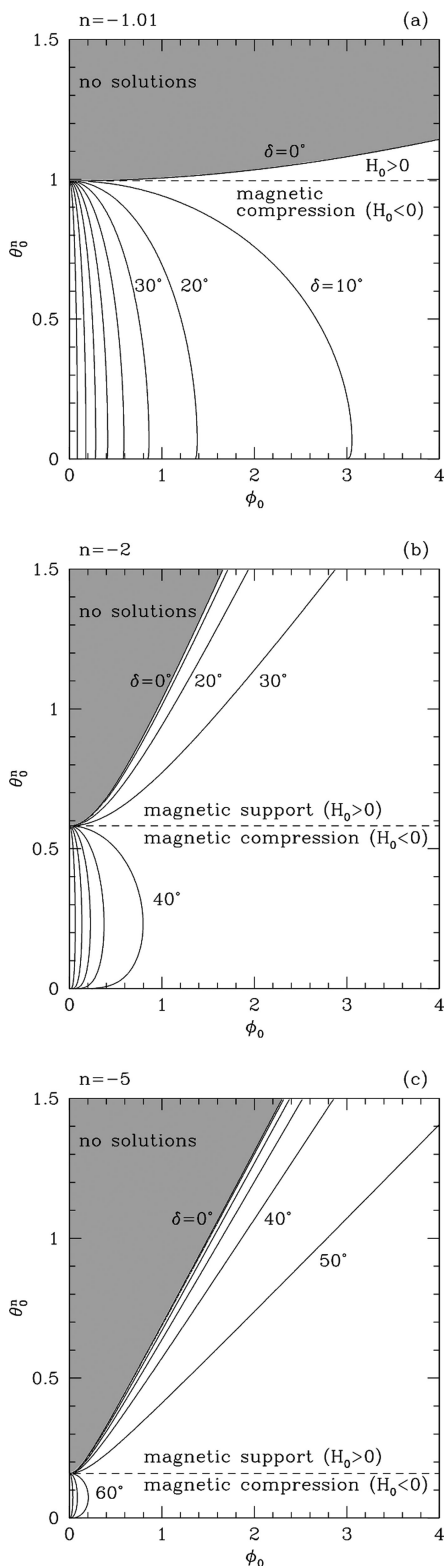
Figure 1. Scale-free solutions in the ϕ_0–θ_0^n plane for $n = 1.01$ (panel a), $n = -2$ (panel b) and $n = -5$ (panel c). The curves are for selected values of the pitch angle δ from $0°$ to $90°$ in steps of $10°$. No solutions exist above the $\delta = 0°$ curve, representing models with a pure poloidal field. No solutions exist in the shaded area above this curve. The dashed line is for the pitch angle $\delta_{\rm ff}$, when the field becomes force-free. Above this line, the magnetic field provides support to the cloud ($H_0 > 0$); below the dashed line, the magnetic field compresses the cloud ($H_0 < 0$).

4.3 Force between magnetized filaments

The magnetic field discussed in the previous sections is generated by electric currents flowing in the filaments. A toroidal field $B_\varphi(\varpi)$, for instance, is associated with an electric current $I(\varpi)\hat{e}_z$ flowing along the filament given by

$$I(\varpi) = \frac{c}{2} \int_0^\varpi [\nabla \times (B_\varphi \hat{e}_\varphi)]\varpi \, d\varpi = \frac{c}{2} \varpi B_\varphi(\varpi). \tag{57}$$

Thus, two parallel filaments, separated by a distance d larger than their radii ϖ_s, behave as two electric wires and exert on each other an electromagnetic force (per unit length) $\boldsymbol{F}_{\rm em}$, repulsive if the currents are aligned, attractive if they are anti-aligned, given by

$$\boldsymbol{F}_{\rm em} = \frac{2I_1 I_2}{c^2 d} \, \hat{\boldsymbol{e}}_\varpi. \tag{58}$$

This electromagnetic force scales as the gravitational force (per unit length) $\boldsymbol{F}_{\rm g}$ between the two filaments,

$$\boldsymbol{F}_{\rm g} = \frac{2G\mu_1 \mu_2}{d} \, \hat{\boldsymbol{e}}_\varpi, \tag{59}$$

where μ is the mass per unit length. Therefore, their ratio is independent on the filaments separation

$$\mathcal{R} \equiv \frac{|\boldsymbol{F}_{\rm em}|}{|\boldsymbol{F}_{\rm g}|} = \frac{I_1 I_2}{c^2 G \mu_1 \mu_2} \sim \left(\frac{I}{cG^{1/2}\mu}\right)^2, \tag{60}$$

where the last approximation assumes that the two filaments have similar properties. According to equation (57), the electric current is zero on the axis and equal to $c\varpi_s B_{\varphi, s}/2$ on the surface (in our scale-free models for the filaments' envelopes, in which ϖB_φ increases outwards, the electric current is maximum at the surface). Taking the average, we can set $I \approx c\varpi_s B_{\varphi, s}/4$, to obtain

$$\mathcal{R} \approx \frac{1}{16} \left(\frac{\varpi_s B_{\varphi, s}}{G^{1/2}\mu}\right)^2. \tag{61}$$

Inserting numerical values,

$$\mathcal{R} \approx 22 \left(\frac{\varpi_s}{1\,{\rm pc}}\right)^2 \left(\frac{B_{\varphi, s}}{10\,\mu{\rm G}}\right)^2 \left(\frac{\mu}{10\,{\rm M}_\odot\,{\rm pc}^{-1}}\right)^{-2}. \tag{62}$$

The largest uncertainty on this result (in addition to the extreme idealization of the picture) comes from the difficulty of estimating the filament's outer radius ϖ_s (see discussion in Arzoumanian et al. 2011) and the corresponding value of the (toroidal) magnetic field. Nevertheless the non-negligible numerical value of $\mathcal{R}$ indicates that the electromagnetic forces may play a role as important as gravity in the interaction between magnetized filaments.

5 CONCLUSIONS

We have derived general equations for magnetized filamentary clouds with a polytropic equation of state, assuming cylindrical symmetry and magnetostatic equilibrium. The problem can be formulated in terms of two partial differential equations for four unknowns: the density ρ, the flux function Φ for the poloidal field, and two functions of Φ, namely the enthalpy $H(\Phi)$ and the toroidal field function $\Psi(\Phi)$. Solutions can only be obtained by making additional assumptions, due to the lack of information on the previous evolution of the system. These additional assumptions take usually the form of specific choices of the dependence of the two component of the field on density and/or radius (e.g. Stódołkiewicz 1963; Talwar & Gupta 1973; Fiege & Pudritz 2000). In this work, we have avoided assumptions of this kind, analysing the properties of the models in the region near the axis (the filament's 'core') where

the boundary conditions imposed by symmetry requirements determine the behaviour of the solutions, and at large radii, where the solutions are expected to approach a scale-free form for $n \leq 1$. In this paper, we have explored the range from a 'logatropic' ($n = -1$, or $\gamma_p = 0$) to an 'isothermal' ($n \to -\infty$, or $\gamma_p = 1$) equation of state. In this range, all variables have a power-law behaviour with profiles that become flatter as the equation of state becomes softer. As the polytropic exponent γ_p decreases from 1 to 0, the power-law exponents range from -2 to -1 for the density and from -1 to 0 for the magnetic field.

Depending on the power-law slope, the magnetic field affects the radial density profile of the cloud in opposite ways. In the range $n \leq -1$, depending on the relative strength of the toroidal and poloidal components, the magnetic field can either support or compress the cloud (or be force-free). Pure poloidal fields, or with small toroidal components (small pitch angle δ) provide support to the cloud ($H_0 > 0$), allowing higher values of the envelope density θ_0^n than those resulting from thermal support alone. By increasing the strength of the toroidal component ($\alpha^2 > 0$), the effect of the field becomes extremely sensitive to the field strength ϕ_0: a small change in ϕ_0 changes the sign of the Lorentz force, from supporting to squeezing the cloud. In the latter case, the density of the envelope is lower than the corresponding value in a non-magnetized filament. The confining effect of the field is enhanced for softer equations of state, because the poloidal component becomes increasingly uniform. In particular, for a logatropic equation of states, all scale-free solutions are characterized by a Lorentz force directed inwards, and their density is lower than in the non-magnetic case. Conversely, all scale-free solutions converge to zero density in the limit of an isothermal equation of state, because, as shown in Paper I, the 'natural' asymptotic power-law behaviour of an isothermal cylinder is reached only at infinite radius, where the density is zero.

Within the limits of the idealized scale-free models for magnetized filaments presented in this paper, our results suggest that a measure of the pitch angle of the magnetic field associated with filaments can provide a way to discriminate filaments that are compressed by the field from those that are supported. This can be accomplished by comparing the direction of the magnetic field around a filament, as traced by optical/near-infrared polarization, to the direction of the field within the filament, as traced by submillimetre polarization. Preliminary results from the *Planck* satellite (Adam et al. 2014) suggest that the field direction changes from the diffuse to the molecular gas, but the actual amount of field twisting in a filament remains uncertain (see discussion in Section 1). High-resolution observations of polarized dust emission inside the filaments (e.g. with atacama large millimeter/submillimeter array) are needed to assess the role of large- and small-scale magnetic fields in their formation and evolution.

Finally, the magnetization of interstellar filaments implies the presence of electric currents flowing along and/or around them, producing attractive (or repulsive) electromagnetic forces that enhance (or dilute) their gravitational field and may affect their interactions.

ACKNOWLEDGEMENTS

REFERENCES

Adam R. et al., 2014, preprint (arXiv:1409.6728)
Arzoumanian D. et al., 2011, A&A, 529, L6
Carlqvist P., Kristen H., Gahm G. F., 1998, A&A, 332, L5
Chandrasekhar S., Fermi E., 1953, ApJ, 118, 116
Falgarone E., Pety J., Phillips T. G., 2001, ApJ, 555, 178
Fiege J. D., Pudritz R. E., 2000, MNRAS, 311, 85
Gahm G. F., Carlqvist P., Johansson L. E. B., Nikolić S., 2006, A&A, 454, 201
Galli D., Lizano S., Li Z. Y., Adams F. C., Shu F. H., 1999, ApJ, 521, 630
Goodman A. A., Bastien P., Menard F., Myers P. C., 1990, ApJ, 359, 363
Goodman A. A., Jones T. J., Lada E. A., Myers P. C., 1992, ApJ, 399, 108
Hily-Blant P., Falgarone E., Pineau Des Forêts G., Phillips T. G., 2004, Ap&SS, 292, 285
Li H.-b., Fang M., Henning T., Kainulainen J., 2013, MNRAS, 436, 3707
Li Z.-Y., Shu F. H., 1996, ApJ, 472, 211
Lizano S., Shu F. H., 1989, ApJ, 342, 834
Low B. C., Lou Y. Q., 1990, ApJ, 352
Lundquist S., 1950, Ark. Fys., 2, 361
Matthews B. C., Fiege J. D., Moriarty-Schieven G., 2002, ApJ, 569, 304
Moneti A., Pipher J. L., Helfer H. L., McMillan R. S., Perry M. L., 1984, ApJ, 282, 508
Nagasawa M., 1987, Prog. Theor. Phys., 77, 635
Nakamura F., Hanawa T., Nakano T., 1993, PASJ, 45, 551
Palmeirim P. et al., 2013, A&A, 550, A38
Shu F. H., 1992, The Physics of Astrophysics, Vol. II: Gas Dynamics. University Science Books, Mill Valley, CA, p. 320
Sood N. K., Singh K., 2004, Ap&SS, 289, 55
Stódółkiewicz J. S., 1963, Acta Astron. 13, 1
Sugitani K. et al., 2011, ApJ, 734, 63
Talwar S. P., Gupta A. K., 1973, Ap&SS, 23, 347
Toci C., Galli D., 2015, MNRAS, 446, 2110 (Paper I)
Tomisaka K., 2014, ApJ, 785, 24

This paper has been typeset from a TeX/LaTeX file prepared by the author.